

A passive dynamic walking robot that has a deterministic nonlinear gait

Max J. Kurz^{a,*}, Timothy N. Judkins^b, Chris Arellano^a, Melissa Scott-Pandorf^a

^aLaboratory of Integrated Physiology, Department of Health and Human Performance, University of Houston, 3855 Holman Street, Garrison Room 104, Houston, TX 77204-6015, USA

^bDepartment of Physical Therapy and Rehabilitation Science, University of Maryland School of Medicine, Baltimore, MD, USA

Accepted 12 January 2008

Abstract

There is a growing body of evidence that the step-to-step variations present in human walking are related to the biomechanics of the locomotive system. However, we still have limited understanding of what biomechanical variables influence the observed nonlinear gait variations. It is necessary to develop reliable models that closely resemble the nonlinear gait dynamics in order to advance our knowledge in this scientific field. Previously, Goswami et al. [1998. A study of the passive gait of a compass-like biped robot: symmetry and chaos. *International Journal of Robotic Research* 17(12)] and Garcia et al. [1998. The simplest walking model: stability, complexity, and scaling. *Journal of Biomechanical Engineering* 120(2), 281–288] have demonstrated that passive dynamic walking computer models can exhibit a cascade of bifurcations in their gait pattern that lead to a deterministic nonlinear gait pattern. These computer models suggest that the intrinsic mechanical dynamics may be at least partially responsible for the deterministic nonlinear gait pattern; however, this has not been shown for a physical walking robot. Here we use the largest Lyapunov exponent and a surrogation analysis method to confirm and extend Garcia et al.'s and Goswami et al.'s original results to a physical passive dynamic walking robot. Experimental outcomes from our walking robot further support the notion that the deterministic nonlinear step-to-step variations present in gait may be partly governed by the intrinsic mechanical dynamics of the locomotive system. Furthermore the nonlinear analysis techniques used in this investigation offer novel methods for quantifying the nature of the step-to-step variations found in human and robotic gait.

© 2008 Elsevier Ltd. All rights reserved.

Keywords: Walking; Gait; Locomotion; Nonlinear; Variability; Chaos; Robotics

1. Introduction

Human locomotion is typically described as having a periodic movement pattern. For example, it can be readily observed that the legs oscillate to-and-fro with a limit cycle behavior that is similar to the pendulum motions of a clock. Any variations from this periodic pattern have traditionally been considered to be instabilities in the coupling of the components locomotive system, i.e., noise (Hausdorff et al., 1995; Riley and Turvey, 2002). However, recent investigations have indicated that the step-to-step variations that are present in human gait may not be instabilities; rather these variations may have a deterministic structure that is dependent on the biomechanics of the locomotive system (Hausdorff et al., 1995; Dingwell

and Cusumano, 2000; Buzzi et al., 2003; Miller et al., 2006; Stergiou et al., 2004). Currently, we still have limited insight on what variables are actually governing the observed step-to-step variations.

Previous insights on the origin of the nonlinear dynamics of physical systems (i.e., pendulums, magnetic ribbons, lasers, etc.) have come from the analysis of simplified mathematical models that are sufficiently close to the behavior of the real system (Glass, 2001). Full and Koditschek (1999) referred to such simple models as templates. In the case of locomotion, the template has all the joint complexities, muscles and neurons removed. Recently, passive dynamic walking models have proven to be a useful template for the exploration of nonlinear gait dynamics (Garcia et al., 1998; Goswami et al., 1998; Kurz and Stergiou, 2005, 2007a, b). These models consist of an inverted double pendulum system that captures the dynamics of the swing and stance phase of gait (Fig. 1A).

*Corresponding author. Tel.: +1 713 743 2274.

E-mail address: mkurz@uh.edu (M.J. Kurz).

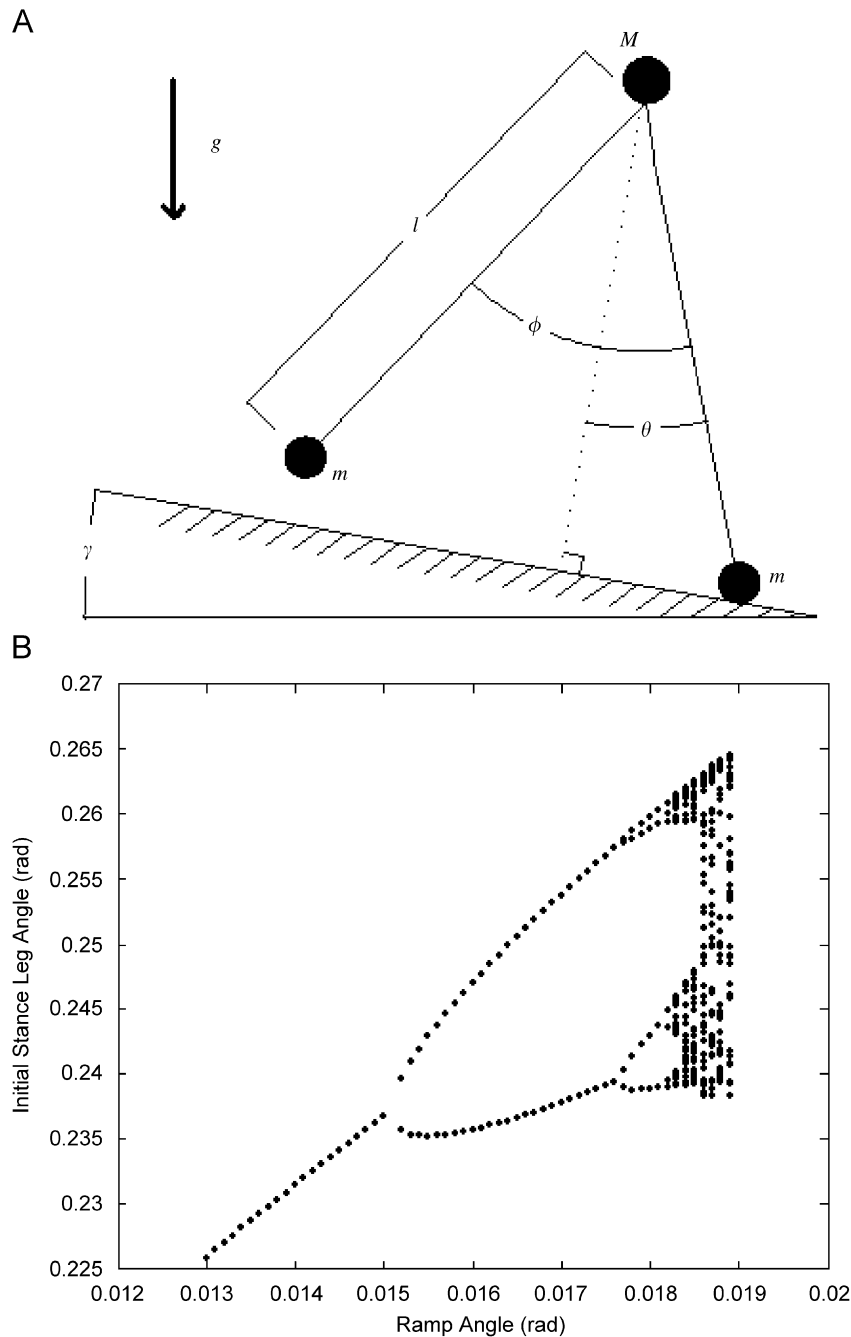


Fig. 1. (A) Passive dynamic walking model that has a nonlinear gait pattern. Further details on the model's equations of motion are found in Garcia et al. (1998). (B) Cascade of bifurcations in the walking model's gait as the ramp angle is inclined. These gaits eventually converge to a deterministic nonlinear gait pattern than is chaotic.

The model maintains a stable walking pattern by introducing energy into the system via a slightly sloped walking surface. As the walking surface angle is increased, there is a cascade of bifurcations in the model's gait pattern that leads to a deterministic nonlinear gait pattern (Fig. 1B) (Goswami et al., 1998; Garcia et al., 1998).

This passive dynamic framework has provided a theoretical basis for building walking robots that have improved our understanding of stable and efficient walking in humans (McGeer, 1990; Collins et al., 2005). Histori-

cally, the analysis of the gait patterns of these walking robots has focused on the periodic nature of the gait pattern. Any variations in the walking robot's gait were considered to be instabilities in the mechanical coupling, i.e., noise. Passive dynamic walking computer models suggest that these variations may not be instabilities, but may arise from the inherent dynamics of the locomotive system (Garcia et al., 1998; Goswami et al., 1998). This notion has yet to be validated in a physical passive dynamic walking robot. Verification of a deterministic nonlinear

gait pattern in a physical passive dynamic walking robot will provide a new theoretical foundation for understanding and modeling the deterministic step-to-step variations found in human locomotion. Here we hypothesize that a simple passive dynamic walking robot can exhibit a deterministic nonlinear gait pattern.

2. Walking robot design

We constructed a simple passive dynamic walking robot that was based on the original work of [Tedrake et al. \(2004\)](#). The robot had two rigid legs, a pin joint between the hips, and wooden feet that were curved in the sagittal and frontal planes. The legs were 0.41 m long and assembled using pre-manufactured aluminum extrusions (80/20, Inc., Columbia City, IN). The spacing between the legs was 0.19 m, and the radius of curvature in the frontal and sagittal planes were approximately 0.15 and 0.25 m, respectively ([Fig. 2](#)).

The curvature of the feet in the frontal plane allowed for the walking robot to avoid collisions at mid-stance by slightly rocking to the side. Walking was initiated by positioning the robot at the top of a treadmill (Biodex, RTM400, Shirley, NY) and giving it a slight push sideways. The treadmill used in this investigation had a 2 HP motor with 4Q-pulse width modulation control that allowed it to operate at low speeds with high accuracy. During locomotion, the robot would rock over the stance leg, and the opposite leg would swing forward taking a step down the treadmill. At foot-strike, the robot would rock onto the opposite foot for the next step of the gait cycle. We evaluated five stable long-term locomotion trials (40–100 steps per trial) from the robot as it walked on the treadmill that operated in reverse (e.g., downhill) at a

speed of 0.04 m/s. The sagittal plane leg kinematics of the walking robot's gait were collected at 60 Hz using a three-dimensional motion capture system (ViconPeak, Centennial, CO).

3. Nonlinear analysis measures

3.1. State space reconstruction

In order to evaluate the nature of the step-to-step variations in the gait pattern, we used standard embedding techniques from nonlinear dynamics to reconstruct the state space of the walking robot's locomotive attractor from the leg angle time series ([Kantz and Schreiber, 2004](#)). The nonlinear analysis techniques used time-lagged copies of the original leg angle time series to reconstruct the state vector that defined the walking robot's locomotive attractor. Eq. (1) presents the reconstructed state vector where $y(t)$ was the reconstructed state vector, $x(t)$ was the original time series data, d_E was the dimension of the vector, and $x(t + T_i)$ was time delay copies of $x(t)$:

$$y(t) = [x(t), x(t + T), x(t + 2T), \dots, x(t + (d_E - 1)T)]. \quad (1)$$

The time delay (T_i) for creating the state vector was determined by estimating when information about the state of the dynamic system at $x(t)$ was different from the information contained in its time-delayed copy using an average mutual information algorithm ([Abarbanel, 1996](#)). Eq. (2) presents the average mutual information algorithm where T was the time delay, $x(t)$ was the original data, $x(t + T)$ was the time delay data, $P(x(t), x(t + T))$ was the joint probability for measurement of $x(t)$ and $x(t + T)$, $P(x(t))$ was the probability for measurement of $x(t)$, and $P(x(t + T))$ was the probability for measurement of $x(t + T)$:

$$I_{x(t), x(t+T)} = \sum P(x(t), x(t + T)) \log_2 \left[\frac{P(x(t), x(t + T))}{P(x(t))P(x(t + T))} \right]. \quad (2)$$

Average mutual information was iteratively calculated for various time delays, and the selected time delay was the first local minimum of the iterative process ([Fig. 3](#)). This selection was based on previous investigations that have determined that the time delay at the first local minimum contains sufficient information about the dynamics of the system to reconstruct the state vector from the measured time series ([Abarbanel, 1996](#)).

3.2. Embedding dimension

We calculated the number of embedding dimensions of the leg angle time series in order to unfold the reconstructed locomotive attractor in an appropriate state space. To unfold the state space, we used a global false nearest neighbors algorithm to systematically inspect $x(t)$, and its neighbors in various dimensions (e.g., dimension = 1, 2, 3, ..., etc.). The appropriate embedding dimension was



Fig. 2. Passive dynamic walking robot developed for this investigation.

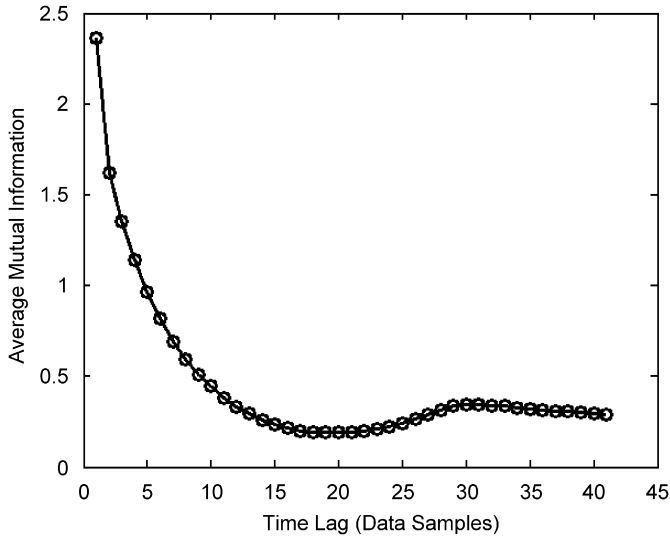


Fig. 3. Exemplary average mutual information curve from the walking robot's gait. The first local minimum of the curve was used to select a time lag for reconstructing the locomotive attractor from the leg angle time series.

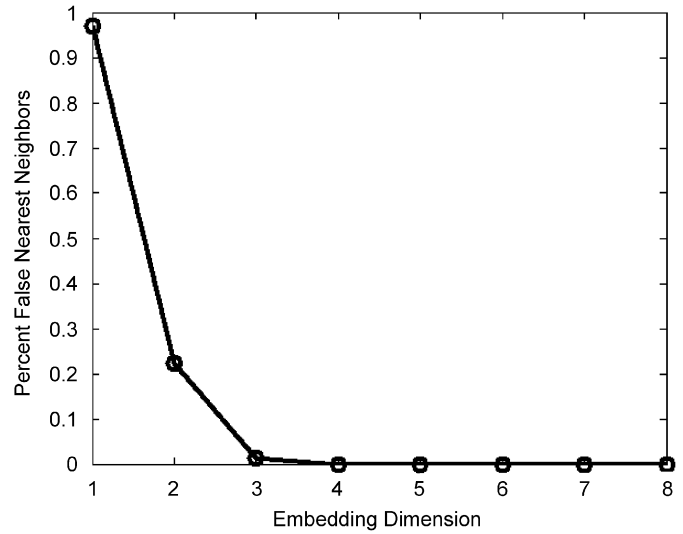


Fig. 4. Exemplary global false nearest neighbors curve from the walking robot's gait. The necessary embedding dimensions for unfolding the locomotive attractor is apparent when the percent false nearest neighbors drops to zero.

identified when the distance between neighboring points in the state space no longer changed with the addition of further dimensions of the state vector. For example, the global false nearest neighbors algorithm compares the points in the attractor at a given dimension d_E

$$y(t) = [x(t), x(t + T), x(t + 2T), \dots, x(t + (d_E - 1), T)] \quad (3)$$

$$y^{NN}(t) = [x^{NN}(t), x^{NN}(t + T), x^{NN}(t + 2T), \dots, x^{NN}(t + (d_E - 1)T)], \quad (4)$$

where $y(t)$ was the current point being considered, and $y^{NN}(t)$ was the nearest neighbor. If the distance between the points at the next dimension (e.g., d_{E+1}) was greater than the distance calculated at the current dimension (e.g., d_E), then the point was considered a false neighbor and further embeddings were necessary to unfold the attractor. The percentage of false nearest neighbors was calculated at higher dimensions until the percent nearest neighbors dropped to zero (Fig. 4). The embedding dimension that had zero percent false nearest neighbors was used to reconstruct the walking robot's locomotive attractor in an appropriate state space.

3.3. Lyapunov exponent

The largest Lyapunov exponent was calculated to determine the nonlinear structure of the reconstructed attractor. Lyapunov exponents quantify the average rate of separation or divergence of points in the attractor over time (Kantz and Schreiber, 2004; Abarbanel, 1996; Rosenstein et al., 1993). A periodic system will have no divergence of points in the attractor, while a nonlinear system will have some divergence between two neighboring points as time progresses. Fig. 5A presents a hypothetical

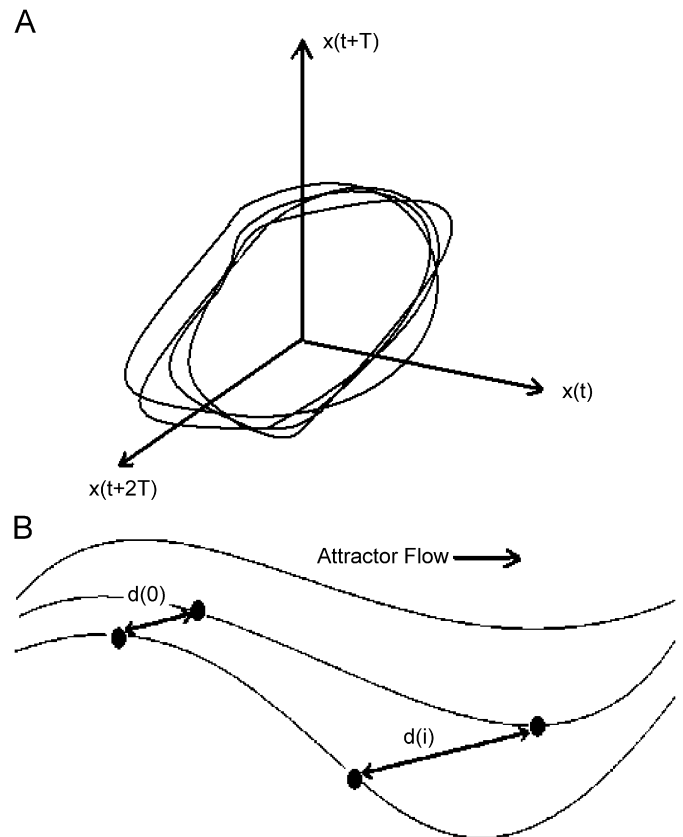


Fig. 5. (A) Hypothetical reconstructed nonlinear attractor. (B) Zoomed-in window of the reconstructed attractor where $s(0)$ is the initial Euclidean distance between two neighboring points in the attractor and $s(i)$ is the Euclidean distance between the two points i times later.

reconstructed nonlinear attractor, and Fig. 5B is an expanded view of a portion of the reconstructed attractor. Fig. 5B depicts two neighboring points in the reconstructed

attractor that are separated by an initial distance of $d(0)$. As time progresses, the two points diverge rapidly and are separated by a distance of $d(i)$. The Lyapunov exponent is a measure of the logarithmic divergence of the pairs of neighboring points in the attractor over time.

Eq. (5) is the algorithm for determining the Lyapunov exponent where λ is the Lyapunov exponent, Δt is the sampling period, M is the number of points in the attractor considered, $d_j(0)$ is the initial Euclidean distance between the j neighbors, and $d_j(i)$ it is the Euclidean distance between the j neighbors i times later (Rosenstein et al., 1993):

$$\lambda(i) = \frac{1}{i \cdot \Delta t} \left[\frac{1}{M-i} \sum_{j=1}^{M-i} \ln \frac{d_j(i)}{d_j(0)} \right]. \quad (5)$$

The largest Lyapunov exponent was estimated by plotting the divergence curve which consists of average rate of divergence of neighboring points in the attractor as a function of time (Fig. 6). The largest Lyapunov exponent of the walking robot was estimated by using a least squares algorithm to calculate the slope of the linear region of the divergence curve that exists between zero and the second stride (Fig. 6) (Rosenstein et al., 1993).

We used a pseudo periodic surrogation (PPS) algorithm to determine if the calculated Lyapunov exponent was related to a deterministic or stochastic process (Miller et al., 2006; Small and Tse, 2002). The PPS algorithm generates a surrogate of the original time series that preserves the inherent periodic components while destroying the nonlinear structure. The structure of the surrogate followed the same vector field as the original time series, but was contaminated with noise. If fluctuations in the original time series have deterministic features, these

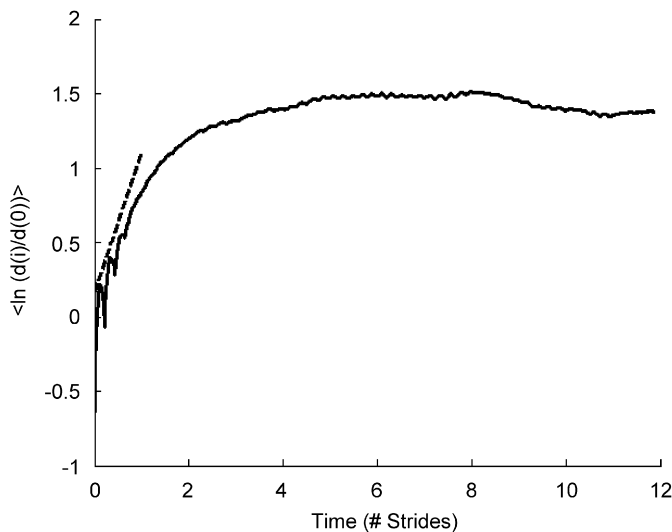


Fig. 6. Exemplary divergence curve from the walking robot's gait. The abscissa of the divergence curve was normalized by multiplying it by the average stride frequency of the walking robot. The largest Lyapunov exponent is estimated from the slope of a line fit to the linear region of the divergence curve that exists from zero to second stride.

features will be destroyed in the surrogate. If the variations in the time series are random noise, the surrogate will be no different from the original time series. The largest Lyapunov exponents were calculated for the original time series (λ_{orig}) and the surrogate (λ_{surr}) to test if the nonlinear structure of the original time series was noise or a deterministic nonlinear pattern. The nonlinear variations in the walking robot's gait are deterministic if the largest Lyapunov exponent of the original time series is statistically different from the largest Lyapunov exponent of the surrogate time series. Statistical analysis was conducted at an alpha level of 0.05.

4. Experimental results

Fig. 7 depicts an exemplary leg angle time series (Fig. 7A) and projection of the walking robot's reconstructed attractor (Fig. 7B). Inspection of Fig. 7A demonstrates that the step-to-step variations in the leg angle were not strictly

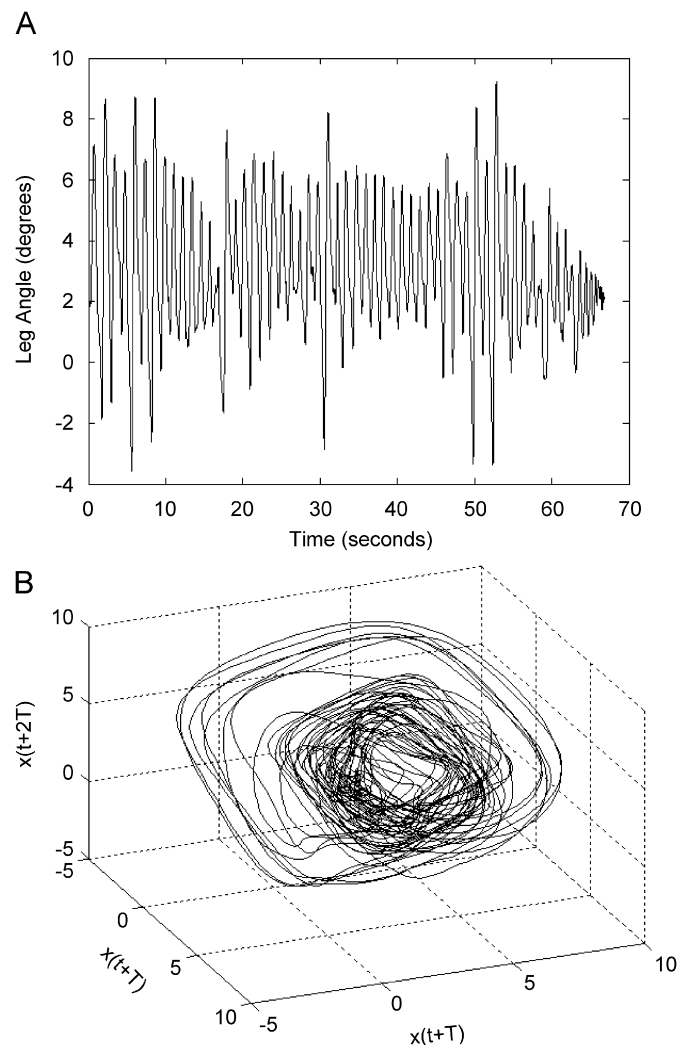


Fig. 7. (A) Exemplary leg angle time series from the robot walking on the slightly sloped and moving treadmill. (B) Projection of the walking robot's reconstructed locomotive attractor.

periodic; rather they had a stationary nonlinear pattern. The time lag used to reconstruct the walking robot's locomotive attractors from the walking trials was 16 ± 0.8 data samples, and the number of embedding dimensions was four. λ_{surr} was significantly ($p = 0.03$) different from λ_{orig} ($\lambda_{\text{surr}} = 1.14 \pm 0.2$; $\lambda_{\text{orig}} = 0.63 \pm 0.2$). This indicated that the nonlinear variations in the walking robot's gait pattern were deterministic, and related to the intrinsic dynamics of the walking robot.

5. Discussion

Our results provide further support for the notion that a passive dynamic walking robot can exhibit a deterministic nonlinear gait. Since the walking robot was completely passive (i.e., no control system), the deterministic step-to-step variations were likely a result of the mechanical coupling and passive dynamics of the walking robot. In human locomotion, we cannot confirm if the nonlinear variations arise from the neurological or mechanical components of the neuromuscular system; however, the results presented here imply that the passive dynamics may play some role in the observed deterministic nonlinear pattern. Our future investigations are directed towards further exploring how the mechanics of the locomotive system may influence the step-to-step nonlinear variations.

Although the treadmill used in this investigation was designed by the manufacture to operate accurately at low speeds, we cannot eliminate the possibility that minute fluctuations in belt speed may have influenced or contribute to the deterministic structure apparent in the gait cycle of the robot. However, the outcomes of our experiment are similar to what has been previously presented in the original passive dynamic computer simulations of Garcia et al. (1998) and Goswami et al. (1998). Since it has been well demonstrated that passive dynamic walking computer models have a deterministic nonlinear gait pattern, we suggest that the deterministic fluctuations seen in the gait pattern of our robot were due to the mechanics of the system rather than the treadmill.

The passive dynamic walking robot presented in this investigation was highly simplified compared to the human locomotive system and walked much slower than a human. This limits our ability to definitively extending the results presented here to human walking. However, it has been previously demonstrated that through this simplification that passive dynamic walking robots have advanced our insight on the biomechanics of human locomotion (Collins et al., 2005). We argue that this is the case here, where our simplified walking robot has provided further verification that deterministic variations in the gait pattern can arise from the mechanical constructs of the locomotive system.

Previous investigations have indicated that a positive Lyapunov exponent may be a signature of a chaotic system (Abarbanel, 1996). A chaotic system's behavior appears to be random and unstable because of the exponential separation of neighboring points in the attractor. However,

unlike random systems, a chaotic system is stable and has deterministic variations. The difficulty in using the largest Lyapunov exponent to quantify the presence of a chaotic pattern is that both random and chaotic systems have a positive Lyapunov exponent due to the presence of the rapid separation of neighboring points in the attractor (Kantz and Schreiber, 2004). We checked the nature of the divergence of the neighboring points in the attractor using the PPS algorithm. Our surrogation tests indicated that the fluctuation in the walking robot's gait were not random instabilities in the walking robot's dynamics. The presence of a positive Lyapunov exponent and a significant difference in the attractor dynamics from the surrogate suggests that our walking robot has a chaotic pattern (Miller et al., 2006; Small and Tse, 2002). Previous results from passive dynamic computer models have indicated that the basin of attraction for chaotic gait is quite large and possibly more stable because multiple types of gaits are available in the attractor (Garcia et al., 1998). Therefore, walking with a chaotic gait may provide the locomotive system with greater flexibility, because it may have the ability to adapt to external perturbations and changes in the walking environment. However, this theoretical concept still need to be further tested and verified.

In our previous walking computer models, we have demonstrated that hip joint actuations applied during the swing phase and toe-off impulses applied at the end of the stance phase could be used to transition to stable gaits that were embedded within the chaotic attractor (Kurz and Stergiou, 2005, 2007a, b). We inferred that this transition flexibility was due to the fact that multiple points found in a chaotic attractor have both unstable and stable manifolds (Abarbanel, 1996; Shinbrot et al., 1993; Ott et al., 1990; Starrett and Tagg, 1995). Small perturbations that are applied along the unstable manifold can be used to drive the system to stable trajectories that are embedded in the chaotic attractor. This property has been well demonstrated in other physical systems such as pendulums and lasers (Abarbanel, 1996; Shinbrot et al., 1993; Starrett and Tagg, 1995). The ability to transition to various stable patterns embedded in the chaotic attractor demonstrates ultimate flexibility and may provide the locomotive system a means to adapt to the ever changing walking environment. Since our walking robot appears to have a chaotic gait, it is possible that it may also be able to demonstrate the ability to transition to stable gaits embedded within the chaotic attractor. Our future research is directed toward testing this theoretical concept by developing walking robots that use joint actuation to transition the locomotive system to gaits embedded within the chaotic attractor.

6. Conclusions

Our results support the original work of Garcia et al. (1998) and Goswami et al. (1998) and further validate the notion that a deterministic nonlinear gait is possible in

a passive dynamic walking robot. Our methods were novel in that we utilized the largest Lyapunov exponent and a surrogate analysis method to derive these conclusions. Further use of these nonlinear tools may provide additional insight on the nature of the step-to-step fluctuations present in human and robotic locomotion. The results presented in this investigation imply that the gait pattern of the walking robot may have a chaotic pattern. Our future research will explore if the results from our previous simulations can be extended to walking robots to improve stability in unstable walking environments.

Conflict of interest statement

There are no financial and personal relationships with the authors of this manuscript or the organization that may have biased the work presented here.

Acknowledgment

Funding provided by the Texas Learning and Computational Center Grant awarded to MJK.

References

- Abarbanel, H.D.I., 1996. *Analysis of Observed Chaotic Data*. Springer, New York.
- Buzzi, U.H., Stergiou, N., Kurz, M.J., Hageman, P.A., Heidel, J., 2003. Nonlinear dynamics indicates aging affects variability during gait. *Clinical Biomechanics* 18, 435–443.
- Collins, S., Ruina, A., Tedrake, R., Wisse, M., 2005. Efficient bipedal robots based on passive-dynamic walkers. *Science* 307, 1082–1085.
- Dingwell, J.B., Cusumano, J.P., 2000. Nonlinear time series analysis of normal and pathological human walking. *Chaos* 10 (4), 848–863.
- Full, R.J., Koditschek, D.E., 1999. Templates and anchors: neuromechanical hypotheses of legged locomotion on land. *Journal of Experimental Biology* 202, 3325–3332.
- Garcia, M., Chatterjee, A., Ruina, A., Coleman, M., 1998. The simplest walking model: stability, complexity, and scaling. *Journal of Biomechanical Engineering* 120 (2), 281–288.
- Glass, L., 2001. Synchronization and rhythmic processes in physiology. *Nature* 410, 277–284.
- Goswami, A., Thuirot, B., Espiau, B., 1998. A study of the passive gait of a compass-like biped robot: symmetry and chaos. *International Journal of Robotic Research* 17 (12).
- Hausdorff, J.M., Peng, C.K., Ladin, Z., Wei, J.Y., Goldberger, A.L., 1995. Is walking a random walk? Evidence for long-range correlations in stride interval of human gait. *Journal of Applied Physiology* 78 (1), 349–358.
- Kantz, H., Schreiber, T., 2004. *Nonlinear Time Series Analysis*, second ed. Cambridge University Press, New York.
- Kurz, M.J., Stergiou, N., 2005. An artificial neural network that utilizes hip joint actuations to control bifurcations and chaos in a passive dynamic bipedal walking model. *Biological Cybernetics* 93 (3), 213–221.
- Kurz, M.J., Stergiou, N., 2007a. Hip actuations can be used to control bifurcations and chaos in a passive dynamic walking model. *Journal of Biomechanical Engineering* 129 (2), 216–222.
- Kurz, M.J., Stergiou, N., 2007b. Do propulsive forces influence the nonlinear structure of locomotion? *Journal of Neuroengineering and Rehabilitation* 4 (30).
- McGeer, T.A., 1990. Passive dynamic walking. *International Journal of Robotic Research* 9 (2), 62–82.
- Miller, D.J., Stergiou, N., Kurz, M.J., 2006. An improved surrogate method for detecting the presence of chaos in gait. *Journal of Biomechanics* 39, 2873–2876.
- Ott, E., Grebogi, C., Yorke, J.A., 1990. Controlling chaos. *Physical Review Letters* 64 (11), 1196–1199.
- Riley, M.A., Turvey, M.T., 2002. Variability and determinism in motor behavior. *Journal of Motor Behavior* 34 (2), 99–125.
- Rosenstein, M.T., Collins, J.J., De Luca, C.J., 1993. A practical method for calculating largest Lyapunov exponents from small data sets. *Physica D* 65, 117–134.
- Shinbrot, T., Grebogi, C., Ott, E., Yorke, J.A., 1993. Using small perturbations to control chaos. *Nature* 363, 411–417.
- Small, M., Tse, C., 2002. Applying the method of surrogate data to cyclic time series. *Physica D* 164, 187–201.
- Starrett, J., Tagg, R., 1995. Control of a chaotic parametrically driven pendulum. *Physical Review Letters* 74 (11), 1974–1977.
- Stergiou, N., Buzzi, U.H., Kurz, M.J., Heidel, J., 2004. Nonlinear tools in human movement. In: Stergiou, N. (Ed.), *Innovative Analysis of Human Movement*. Human Kinetics, Champaign, IL.
- Tedrake, R., Zhang, T., Fong, M., Seung, H.S., 2004. Actuation a simple 3D passive walker. *Proceedings of the IEEE International Conference on Robotics and Automation (ICRA)* 5, 4656–4661.